

Comparing the Ancient Star Formation Histories of the Magellanic Clouds^{*}

Daniel R. Weisz¹ †, Andrew E. Dolphin², Evan D. Skillman³, Jon Holtzman⁴,
Julianne J. Dalcanton¹, Andrew A. Cole⁵, Kyle Neary³

¹*Department of Astronomy, Box 351580, University of Washington, Seattle, WA 98195*

²*Raytheon, 1151 E. Hermans Road, Tucson, AZ 85756*

³*Minnesota Institute for Astrophysics, University of Minnesota, 116 Church Street SE, Minneapolis, MN 55455, USA*

⁴*Department of Astronomy, New Mexico State University, Box 30001, 1320 Frenger St., Las Cruces, NM 88003*

⁵*School of Mathematics and Physics, University of Tasmania, Hobart, Tasmania, Australia*

15 March 2022

ABSTRACT

We present preliminary results from a new Hubble Space Telescope (HST) archival program aimed at tightly constraining the ancient (> 4 Gyr ago) star formation histories (SFHs) of the field populations of the SMC and LMC. We demonstrate the quality of the archival data by constructing HST/WFPC2-based color-magnitude diagrams (CMDs; $M_{F555W} \sim +8$) for 7 spatially diverse fields in the SMC and 8 fields in the LMC. The HST-based CMDs are > 2 magnitudes deeper than any from ground based observations, and are particularly superior in high surface brightness regions, e.g., the LMC bar, which contain a significant fraction of star formation and are crowding limited from ground based observations. To minimize systematic uncertainties, we derive the SFH of each field using an identical maximum likelihood CMD fitting technique. We then compute an approximate mass weighted average SFH for each galaxy. From the average SFHs, we find that both galaxies lack a dominant burst of early star formation in the MCs. From 10-12 Gyr ago, we find that the LMC experienced a period of enhanced stellar mass growth relative to the SMC. Similar to some previous studies, we find two notable peaks in the SFH of the SMC at ~ 4.5 and 9 Gyr ago, which could be due to repeated close passages with the LMC, implying an interaction history that has persisted for at least 9 Gyr. We find little evidence for strong periodic behavior in the lifetime SFHs of both MCs, suggesting that repeated encounters with the Milky Way are unlikely. Beginning ~ 3.5 Gyr ago, both galaxies show sharp increases in their SFHs, in agreement with previous studies. Subsequently, the SFHs track each other remarkably well. Spatial variations in the SFH of the SMC are consistent with a picture where gas was driven into the center of the SMC ~ 3.5 Gyr ago, which simultaneously shut down SF in the outer regions while dramatically increasing the star formation rate in the center. In contrast, the LMC shows little spatial variation in its ancient SFH. The planned additional analysis of HST pointings at larger galactocentric radii will allow us to make more confident statements about spatial variations in the ancient SFHs of the SMC and LMC.

Key words: galaxies: stellar content, galaxies: dwarf, Magellanic Clouds, color-magnitude diagrams (HR diagram)

1 INTRODUCTION

The Magellanic Clouds (MCs) are among the best studied galaxies in the universe. Their close proximity has motivated detailed observations of their gas, dust, and stellar contents (e.g., Zaritsky et al. 1997; Kim et al. 1998; Zaritsky et al.

^{*} Based on observations made with the NASA/ESA Hubble Space Telescope, obtained from the Data Archive at the Space Telescope Science Institute, which is operated by the Association of Universities for Research in Astronomy, Inc., under NASA contract NAS 5-26555
 † E-mail: dweisz@astro.washington.edu

2002; Stanimirović et al. 2004; Kallivayalil et al. 2006a,b; Meixner et al. 2006; Udalski et al. 2008a,b; Kerber et al. 2009; Gordon et al. 2011; Meixner et al. 2010; Rubele et al. 2012), providing for a holistic understanding of their genesis and evolution. In particular, stars fainter than the oldest main sequence turnoff (MSTO) are readily observable, providing for excellent constraints on the star formation histories (SFHs) of the MCs across all cosmic time. In turn, such SFHs can be used as empirical discriminants between various evolutionary models of the MCs (e.g., Murai & Fujimoto 1980; Lin & Lynden-Bell 1982; Fich & Tremaine 1991; Gardiner et al. 1994; Heller & Rohlfs 1994; Lin et al. 1995; Bekki & Chiba 2005; Besla et al. 2007; Diaz & Bekki 2012; Besla et al. 2010, 2012).

Despite extensive investments in measuring the SFHs of the MCs, our understanding of their ancient SFHs (> 4 Gyr) is surprisingly limited. Most wide-field ground based surveys provide spatially comprehensive coverage, but the resulting color-magnitudes diagrams (CMDs) only extend below the oldest MSTO in the uncrowded outer regions (e.g., Harris & Zaritsky 2004, 2009; Noël et al. 2009; Udalski et al. 2008a,b; Kerber et al. 2009; Saha et al. 2010; Piatti et al. 2012; Rubele et al. 2012), leaving the ancient SFHs of more crowded inner regions highly uncertain. Conversely, others have used the Hubble Space Telescope (HST) to overcome crowding limitations (e.g., Geha et al. 1998; Olsen 1999; Holtzman et al. 1999; Dolphin et al. 2001; Smecker-Hane et al. 2002; McCumber et al. 2005; Cignoni et al. 2012), but such studies typically only consider small numbers of fields, compromising the spatially representative nature of the results. Further, past SFH studies have typically focused on either the SMC or the LMC. The use of different SFH measurement techniques or stellar libraries can introduce systematic offsets, making a comparison between the ancient SFHs of the SMC and LMC difficult.

To remedy these limitations, we have undertaken an HST/Wide Field Planetary Camera 2 (WFPC2; Holtzman et al. 1995) archival study aimed at self-consistently measuring the ancient SFHs of both MCs using over 100 HST fields (HST-AR-12853; PI. D. Weisz). Each of the CMDs selected for this study is significantly deeper than the oldest MSTO and reflect a diverse spatial sampling, enabling a precise and representative measurement of the ancient SFHs of the MCs.

In this paper, we present a first look at results from this ongoing archival program. We have selected 7 spatially diverse HST fields in the SMC and 8 in the LMC to provide a preview of the data quality and to demonstrate the precision of the resulting SFH measurements. We present the CMDs in §2, summarize the method of measuring SFHs in §3, and present and discuss the derived SFHs in §4. The mapping between lookback time and redshift values used in this paper assume a standard WMAP-7 cosmology as detailed in Jarosik et al. (2011).

2 THE DATA

In this program, we utilize photometry and artificial star tests ($\sim 1.2 \times 10^5$ per field) taken from the Local Group Stel-

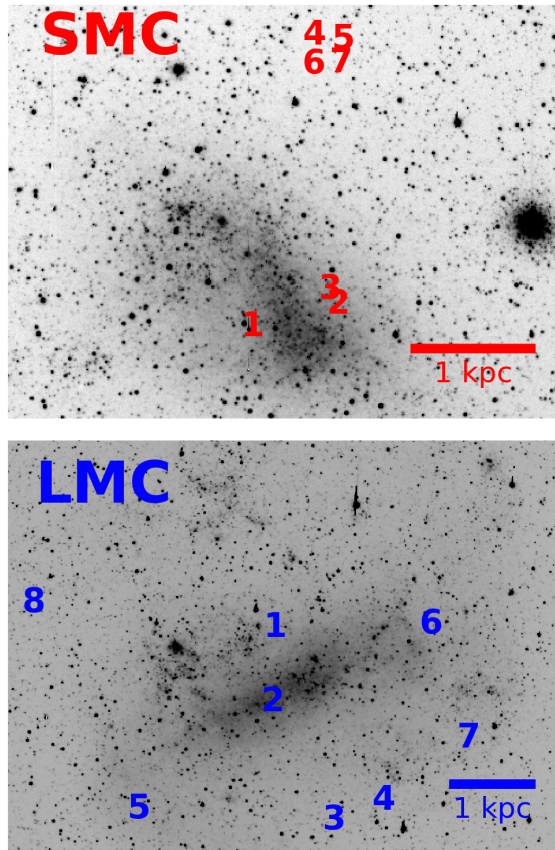


Figure 1. The spatial locations of the HST/WFPC2 fields used in this study for the SMC (top) and LMC (bottom).

lar Photometry Archive¹ (LGSPA; Holtzman et al. 2006). We focus on 7 fields in the SMC and 8 fields in the LMC, which were selected to represent the typical data quality and spatial distribution of the full archival program. The locations of the fields are shown in Figure 1.

We have plotted the CMDs of the 7 SMC fields and 8 LMC fields in Figures 2 and 3, respectively. These CMDs include only well-measured stellar sources, with flag values of 0 or 1 in the LGSPA database. In general, each CMD only contains a few thousand stars, leaving some stellar sequences sparsely populated. However, critical age sensitive features such as the oldest MSTO, sub-giant branch, red giant branch, and luminous main sequence are visually identifiable, providing confidence in the age leverage permitted by the data. To increase reliability of the SFHs, we merged the 4 sparsely populated outer SMC fields for subsequent analysis, after verifying the similarity of their completeness functions.

For both galaxies, HST-based CMDs are > 2 magnitudes deeper than any CMDs from current ground based observations. As discussed in Holtzman et al. (2006) and shown in Figures 2 and 3 and in Table 1, all HST CMDs are highly complete down to their limiting magnitudes, which are in excess of $m_{F555W} = 24-26$, even in the high surface

¹ <http://astronomy.nmsu.edu/holtz/archival/html/lg.html>

Field Number	Field Name	RA (J2000)	DEC (J2000)	Galctocentric Radius (kpc)	70% Completeness		No. Stars in CMD	HST-ID	Foreground A_V (mag)	Differential A_V (mag)	$M_{*,total}$ ($10^5 M_\odot$)
(1)	(2)	(3)	(4)	(5)	M_{F555W} (6)	M_{F814W} (7)	(8)	(9)	(10)	(11)	(12)
SMC-1	u2o903	00:55:37	-73:04:20	0.39	+6.9	+5.6	20315	GO-6229	0.25	...	1.6
SMC-2	u65c06	00:45:41	-72:52:20	0.44	+5.5	+4.0	10563	GO-8654	0.25	...	1.4
SMC-3	u46c01	00:46:40	-72:44:43	0.52	+6.9	+5.6	18294	GO-6860	0.25	...	1.4
SMC-4	u37704	00:45:54	-70:34:43	2.3	+6.6	+4.8	818	GO-6604
SMC-5	u37706	00:48:54	-70:47:43	2.3	+6.6	+4.8	992	GO-6604
SMC-6	u377a4	00:46:06	-70:46:44	2.3	+6.5	+4.8	922	GO-6604
SMC-7	u377a6	00:48:54	-70:32:44	2.3	+6.6	+4.8	783	GO-6604
SMC-4-7	4-7 combined	2.3	+6.5	+4.8	3515	...	0.15	...	0.3
LMC-1	u65006	05:24:06	-68:48:48	0.1	+6.3	+5.0	12971	GO-8676	0.40	0.3	1.4
LMC-2	u2o901	05:24:17	-69:46:50	0.86	+5.8	+5.0	30182	GO-6229	0.25	...	3.7
LMC-3	u4b107	05:14:02	-71:16:44	1.5	+6.3	+5.0	6149	GO-7382	0.20	...	0.6
LMC-4	u65005	05:06:20	-70:58:21	1.6	+6.5	+4.6	6400	GO-8676	0.20	0.3	0.6
LMC-5	u65003	05:45:23	-71:08:45	2.0	+6.4	+5.0	10258	GO-8676	0.45	0.3	1.0
LMC-6	u63s01	05:01:56	-68:37:20	2.0	+6.5	+5.5	10781	GO-8576	0.35	0.3	1.1
LMC-7	u65007	04:54:23	-70:01:58	2.2	+6.4	+5.0	6358	GO-8676	0.35	0.3	0.6
LMC-8	u2o902	05:58:18	-68:20:51	3.4	+7.3	+5.5	3326	GO-6229	0.25	...	0.2

Table 1. The observational properties of the SMC and LMC fields. The extinction values listed in columns 10 and 11 were derived from CMD fitting as described in §3. The total stellar mass formed in each field, i.e., the integral of the SFH, is listed in column 12. As indicated, SMC fields 4-7 were combined to form a single larger field, SMC-4-7.

brightness and crowded LMC bar (e.g., LMC-2). In contrast, the current generation of ground based surveys have typical limiting magnitudes ranging from $m_V \sim 22$ in the disk to $m_V \sim 23$ -24 in the extreme outer halos (e.g., Zaritsky et al. 1997; Harris & Zaritsky 2004, 2009; Noël et al. 2009; Kerber et al. 2009; Udalski et al. 2008a,b; Saha et al. 2010; Rubele et al. 2012). Higher surface brightness regions, such as the LMC bar, tend to have substantially brighter magnitude limits, particularly when accounting for completeness effects (e.g., Harris & Zaritsky 2004, 2009), and are crowding limited from the ground. Overall, HST provides the best possible data for precise ancient SFH measurements in the MCs, particularly in high surface brightness regions, modulo its limited spatial coverage relative to large ground based surveys.

3 MEASURING THE STAR FORMATION HISTORIES

We measured the SFH of each field using MATCH, a maximum likelihood CMD fitting package (Dolphin 2002). Briefly, MATCH takes fixed input parameters (e.g., stellar evolution models, stellar initial mass function) and creates sets of synthetic simple stellar populations (SSPs). These synthetic CMDs are convolved with observational errors from artificial star tests (ASTs) and combined to form a composite synthetic CMD. Linear weights on the SSP CMDs are adjusted to obtain the most likely fit and correspond to the most likely SFH. This process can be repeated at a variety of distance and extinction values to solve for these parameters as well. A more detailed description of MATCH can be found in Dolphin (2002).

We quantified uncertainties in the SFHs using 50 Monte Carlo tests per field for a more detailed discussion of quantifying uncertainties in SFH measurements). Given the comparably deep CMDs in both galaxies and the emphasis on relative SFHs of the two systems, we only computed the random uncertainties due to number of stars, and not the systematic uncertainties due to stellar evolution models. We

refer the reader to Weisz et al. (2011) and Dolphin (2012) for a more detailed discussion of error analysis in CMD-based SFH derivations.

All SFHs presented in this paper used the following parameters: a Kroupa IMF (Kroupa 2001), a binary star fraction of 0.35 with the mass of the secondary drawn from a uniform distribution, and the Padova stellar evolution models (Girardi et al. 2010), with mass limits ranging from 0.15 to 120 M_\odot . We adopted 40 logarithmic time bins between $\log(t) = 6.6$ to 10.15 with a single age bin for the very youngest stars, $\log(t) = 6.6$ -7.4, bins of 0.1 dex for $\log(t) = 7.4$ -9.0, and bins of 0.05 dex for $\log(t) > 9.0$. We allowed the program to search for metallicities between $[M/H] = -2.3$ and 0.1 with a resolution of 0.1 dex. Due to the exquisite depth of the CMDs, we have not placed any prior restrictions on the age-metallicity relationship in the SFH derivation process (e.g., we do not require a monotonically increasing metallicity toward the present). Further, we allowed for a modest metallicity dispersion of 0.15 dex in each time bin, which helps account for potential metallicity spreads at a given age (e.g., da Costa 2002). For SFHs derived from comparably deep CMDs, the resultant chemical evolution models are generally well-constrained and can coarsely discern chemical abundance variations as a function of time (e.g., Gallart et al. 2005; Tolstoy et al. 2009).

We initially allowed the program to solve for the distance to each field. In each case we found the distances to be within ± 0.1 dex of commonly used distances in the literature. For consistency in this preliminary study, we therefore fixed the distance modulus for each field to 18.90 in the SMC and to 18.45 in the LMC (Dolphin et al. 2001; Bono et al. 2008). In the context of the larger archival dataset, we plan to further explore distance measurements from CMD fitting, which may provide orthogonal constraints to current 3D geometrical measurements of the MCs (e.g., Haschke et al. 2012b,c).

We limited our fits to only use stars brighter than the 70% completeness limits as determined by $> 10^5$ artificial star tests per field (see Table 1). For LMC fields 3 and 6, we used slightly brighter limits, in order to exclude faint in-

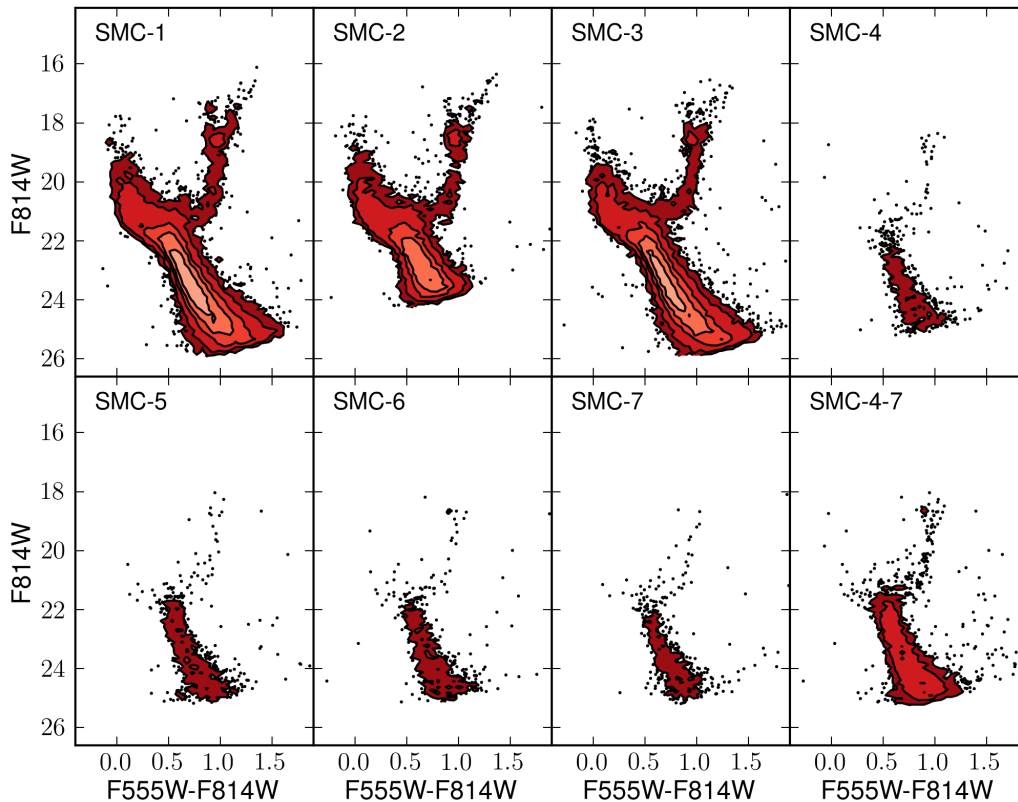


Figure 2. HST/WFPC2-based CMDs of the 7 fields in the SMC. The stellar density contours range from 2 (dark red) to 256 (light red) stars/decimag². The lower right hand panel represents the CMD for the combined outer SMC fields. CMD characteristics such as number of stars and 70% completeness limits are listed in Table 1. These HST-based CMDs are typically > 2 magnitudes deeper than those constructed from ground-based observations, particularly in high surface brightness regions where ground based observations are crowding limited.

involved MS stars that are not included in the Padova models. We also included a foreground CMD of model Milky Way stars following the CMD distributions derived in de Jong et al. (2010).

We allowed MATCH to solve for the line of sight extinction value for each field. The resulting extinction values were comparable with values from the extinction maps based on resolved star de-reddening (Harris et al. 1997; Zaritsky et al. 2002). Including modest amounts of differential extinction in the models improved fits of the elongated red clumps in several of the LMC CMDs (Fields 1, 4-7). Specifically, we found a good differential extinction model to have the following characteristics: 50% of the stars were modeled with $A_V = 0$ and 50% with A_V values evenly distributed between $A_V = 0$ and 0.3.

4 THE ANCIENT STAR FORMATION HISTORIES OF THE MAGELLANIC CLOUDS

4.1 Star Formation Histories of Individual Fields

In Figure 4, we plot the normalized cumulative SFHs, i.e., the fraction of total stellar mass formed prior to a given epoch, for individual fields in the SMC and LMC. For the SMC, we see that each field formed less than 10% of its total

stellar mass prior to ~ 12 Gyr ago. The outer fields (4-7) of the SMC formed the bulk of their stars between ~ 5 and 8 Gyr ago, with little subsequent star formation (SF) until the present, a similar finding to outer area SMC SFHs derived by Dolphin et al. (2001) and Noël et al. (2009). In contrast, the inner fields show a nearly constant SFH from ~ 3.5 -12 Gyr ago, followed by a dramatic increase in SF ~ 3.5 Gyr ago, just when SF in the outer galaxy has shut down. Differences in the SFHs of the inner and outer fields are consistent with previously observed population gradients in the SMC (e.g., Noël et al. 2009).

Like the SMC, most fields in the LMC formed a small percentage of their total mass prior to ~ 12 Gyr ago. Subsequently, most fields experienced a nearly constant SFH until ~ 4 Gyr. At this point, approximately half the fields show signs of an increase in their SFHs, while the other half continued forming stars at a nearly constant rate. There is a slight spatial correlation such that fields close to the bar appear to preferentially show the a rise in star formation, while those farther away do not. However, the majority of the individual field SFHs are consistent at the $1\text{-}\sigma$ level, suggesting a relatively weak population gradient in the LMC over the radial extent subtended by our HST fields, and with previous HST-based studies (e.g., Geha et al. 1998). Our derived SFHs for Fields 2 and 8 are qualitatively similar to previous analysis of the same data (Holtzman et al. 1999).

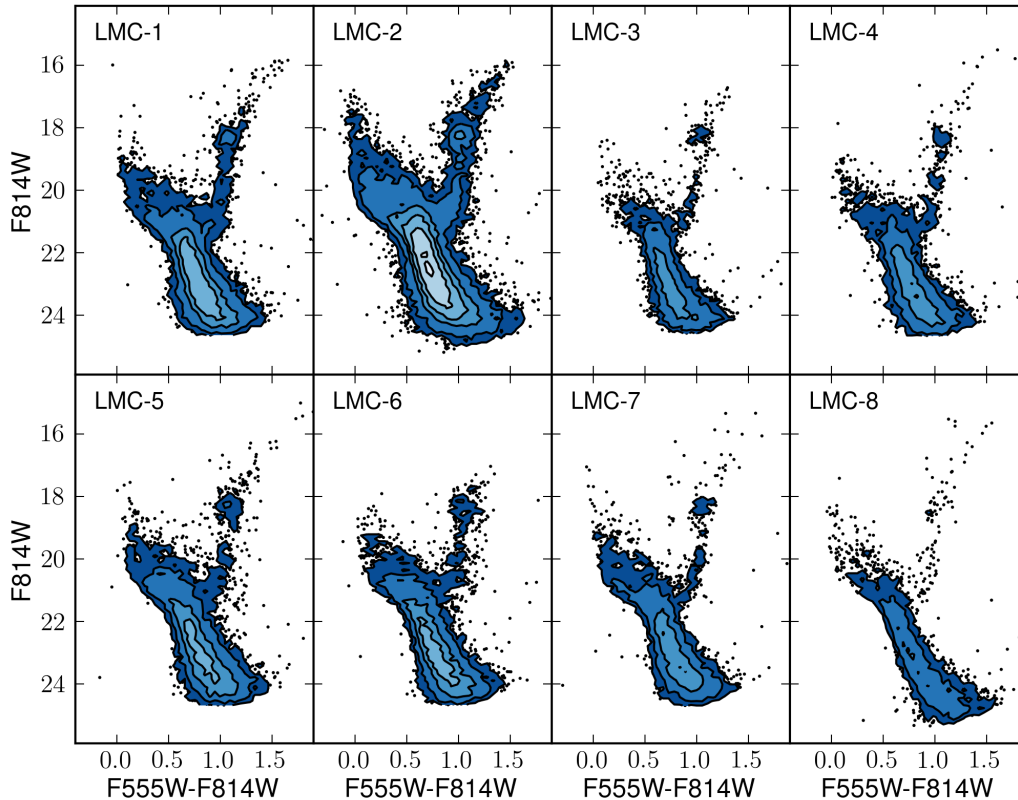


Figure 3. HST/WFPC2-based CMDs of the 8 fields in the LMC. The stellar density contours range from 2 (dark blue) to 512 (white) stars/decimag². CMD characteristics such as number of stars and 70% completeness limits are listed in Table 1. These HST-based CMDs are typically > 2 magnitudes deeper than those constructed from ground-based observations, particularly in high surface brightness regions, e.g., the LMC bar, where ground based observations are crowding limited

4.2 The Mean Star Formation Histories

To compare SFHs between the LMC and SMC, we compute the weighted mean SFH for each galaxy, using the total mass formed in each field (listed in Table 1) as a weight. This approach ensures that the mean SFH is a reasonable proxy for the SFH of the entire galaxy, i.e., integrating over the mean SFH provides a proxy for the total stellar mass of each galaxy, modulo the inherent uncertainty in extrapolating the mean from a small set of fields. More formally, the mean mass weighted SFH from a set of individual fields can be written as

$$\bar{x} = \frac{\sum_i^N w_i x_i}{\sum_i^N w_i}, \quad (1)$$

where x_i is the SFH of a single field and w_i is the total stellar mass formed in that field. Similarly, the $1-\sigma$ uncertainties on the weighted mean SFH are defined to be

$$\sigma(\bar{x}) = \sqrt{\frac{\sum_i^N w_i^2 \sigma_i^2}{\sum_i^N w_i^2}}, \quad (2)$$

where σ_i is the set of uncertainties on the SFH of an individual field. This formalism assumes that the error bars on the SFHs are independent, which is valid in this context as we only consider random uncertainties (which are independent) and not systematic uncertainties (i.e., due to stellar

evolution model selections, which are not independent). We refer the reader to Appendix C of Weisz et al. (2011) and to Dolphin (2012) for further discussion of random and systematic uncertainties in SFHs and their correct propagation for ensemble average SFHs. In addition to propagating uncertainties, we also computed the dispersion in the best fit SFH of each field and added the result in quadrature to the errors in Equation 2.

As shown in Figure 5, the resulting average SFHs of the MCs exhibit several interesting features. First, for ages > 12 Gyr ago, both systems having formed identical fractions ($\sim 10\%$) of their total stellar mass. Second, from ~ 10 -12 Gyr ago, the LMC shows an enhanced period of mass growth relative to the SMC. Third, from ~ 3.5 -12 Gyr ago, both galaxies show mostly constant SFHs, with occasional factor of a few increases compared to the average SFR during this interval (e.g., at ~ 11.5 Gyr ago for the LMC and at ~ 4.5 and 9 Gyr ago for the SMC). Fourth, we find that the SMC and LMC both show sharp increases in their typical SFRs starting ~ 3.5 Gyr ago to the present, such that they form 45-55% of their mass at these recent times. Finally, the SFHs both galaxies track each other very well from 3.5 Gyr ago to the present.

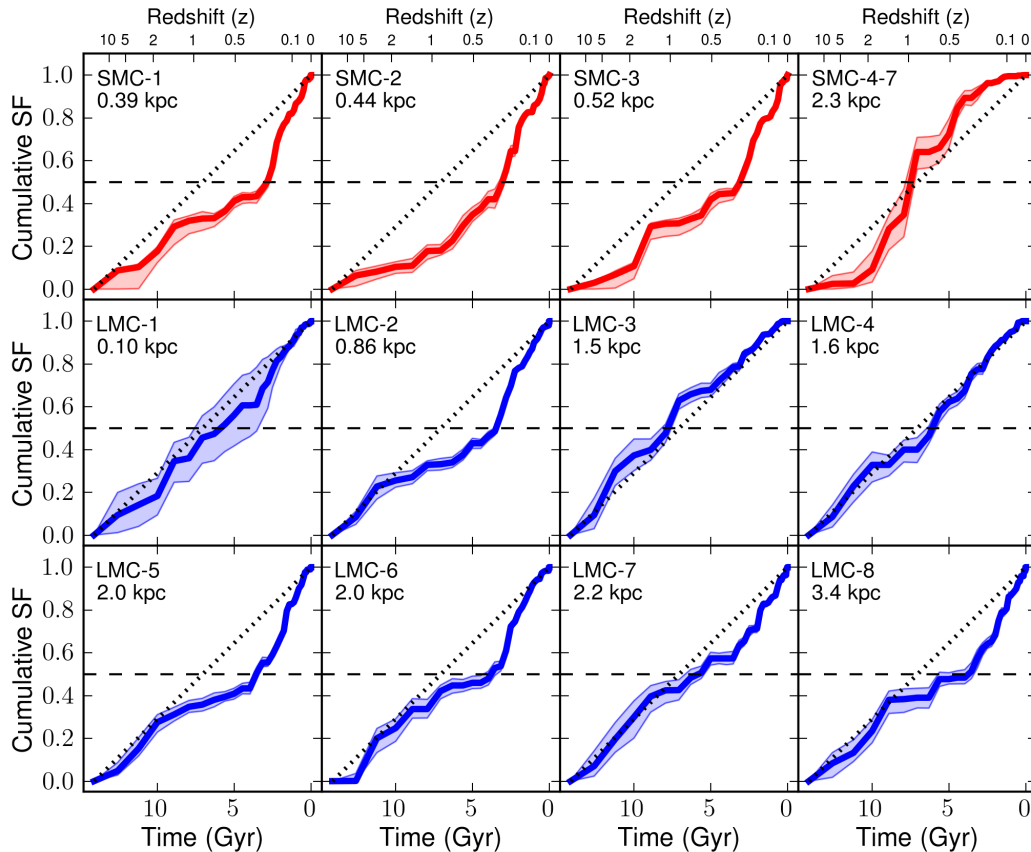


Figure 4. The cumulative SFHs individual fields in the SMC (red) and LMC (blue). The dark red solid line denotes the best fit SFH, while the lighter shaded envelope indicates the $1\text{-}\sigma$ range of the random uncertainties. The dot-dashed line represents the point at which 50% of the total stellar mass formed, and the dotted line reflects a constant SFH.

4.3 Comparison to Previously Derived Star Formation Histories

Our mass weights mean SFHs are similar to SFHs derived in previous studies. In the case of the LMC, previous HST-based SFHs found that the LMC formed 50% of its mass $\sim 5\text{-}6$ Gyr ago and shows a dramatic rise in SFR $\sim 3.5\text{-}4$ Gyr ago (e.g., Geha et al. 1998; Olsen 1999; Holtzman et al. 1999; Smecker-Hane et al. 2002), features also found by Harris & Zaritsky (2009) using shallower data. For the SMC, previous HST-based studies found that the SMC formed $\sim 50\%$ of its stellar mass around $\sim 3\text{-}4$ Gyr ago and experienced a dramatic increase in SF $\sim 3.5\text{-}4$ Gyr ago (e.g., Noël et al. 2009; Cignoni et al. 2012), both similar to results from Harris & Zaritsky (2004). The SFHs of the outer regions ($R > 3$ kpc) of the SMC also show a similar increase in SF $\sim 8\text{-}9$ Gyr ago (e.g., Dolphin et al. 2001; Noël et al. 2009) to our SFH. Completed analysis of the full complement of archival fields will enable more precise global and spatially resolved comparisons to other MC SFH studies.

4.4 Implications for Evolutionary Scenarios of the Magellanic Clouds

Well-constrained SFHs can be useful in discriminating between MCs evolutionary scenarios. Past interactions (or lack

thereof) with one another and/or the Milky Way may have affected the intensity and duration of past star formation events, which can be extracted from precisely constrained lifetime SFHs of both galaxies. In this section, we briefly discuss how our derived SFHs can be used in conjunction with other observations to help discern between various proposed models for the genesis and evolution of the MCs.

At the oldest times (> 12 Gyr ago), the MCs exhibit a level of star formation consistent with a constant lifetime SFH. Such constant star formation at early times makes the MCs standouts among satellites of comparable distance to the Milky Way (e.g., Ursa Minor, Draco), which have predominantly old and truncated SFHs (e.g., Dolphin et al. 2005; Tolstoy et al. 2009). Instead, the constant level of ancient star formation in the MCs more closely resemble isolated dwarfs in the Local Group (e.g., Leo A, IC 1613; Cole et al. 2007; Skillman et al. 2003), each of which have deep CMDs enabling similar SFH derivations (i.e., no age-metallicity restriction was necessary). This finding qualitatively suggests that the MCs were located in a more isolated or possibly field environment at early stages in their evolution. Alternatively, the low levels of star formation may be due to a lack of sufficient fuel at early times. For example, the metallicities of RR Lyrae in the LMC are consistent with an early and rapid chemical enrichment scenario (e.g., Haschke et al. 2012a), which is better matched to an in-

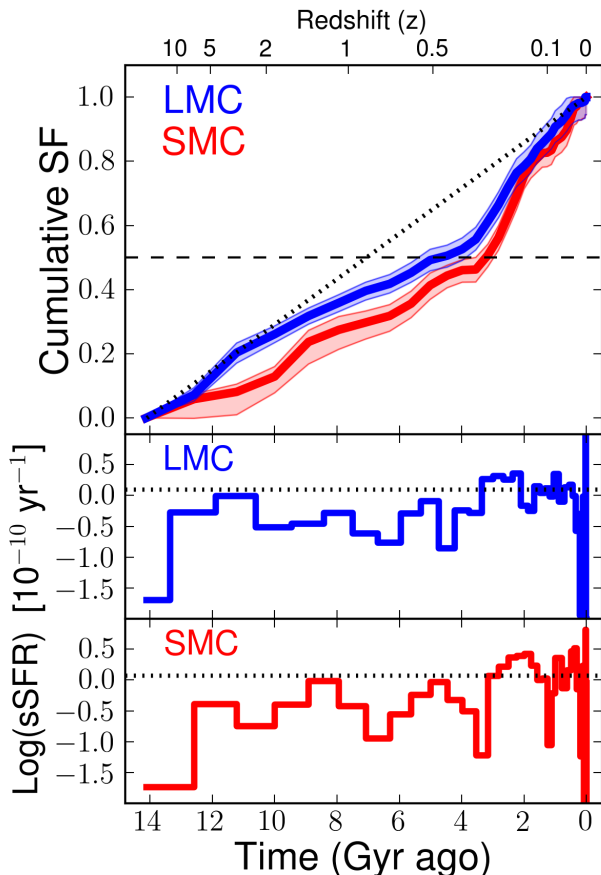


Figure 5. The sample averaged cumulative SFHs for the SMC (red) and LMC (blue) in the top panel and, for increased clarity, the mean specific SFHs in the lower panels. The shaded error envelopes represent the standard error in the mean cumulative SFHs due to random uncertainties and the dispersion in the best fits from the individual SFHs. The black dotted line reflects a constant lifetime SFH, and the dot-dashed line represents the formation of 50% of the total stellar mass. From ~ 3.5 -12 Gyr ago, both the SMC and LMC show constant SFHs at levels lower than the lifetime averages. The SFH of the SMC has two peaks at ~ 4.5 and 9 Gyr ago. Both SFHs show a dramatic increase starting around ~ 3.5 Gyr ago, a feature consistent with previously derived SFHs of the MCs, and are subsequently remarkably similar. The globally representative nature of these SFHs for ages < 2 Gyr are uncertain due to the mixing timescale of young populations and the limited number of HST fields used in this paper.

stantaneous gas recycling model as opposed to significant accretion of lower metallicity material (e.g., Pagel & Tautvaisiene 1998; Carrera et al. 2008). Studies by Piatti et al. (2005) and Carrera et al. (2008) suggest a similar rapid early enrichment scenario is also possible in the SMC.

From ~ 3.5 to 12 Gyr ago, there are interesting features in the SFHs of the MCs. First, from ~ 10 -12 Gyr ago, there is a pronounced difference in the SFHs of the SMC and LMC. Over this interval, the LMC experienced a substantial period of mass growth, forming a significantly larger fraction of its total stellar mass compared to the SMC. This suggests that the LMC may have accreted more material and/or formed stars more efficiently than the SMC at this time. Subsequent

to this interval, the SFHs of the MCs do not exhibit such drastic differences.

Second, from ~ 3.5 and 10 Gyr ago, there are subtle differences between the SFHs of the two galaxies. Over this period, the SFH of the LMC was nearly constant, while the SFH of the SMC appears to have peaks at ~ 4.5 and 9 Gyr ago. These star formation enhancements in the SMC could be the result of interactions with the LMC. Due to the order of magnitude mass difference in the systems, an interaction between the two systems would likely enhance the global SFR of the SMC, but would not similarly affect the LMC (e.g., Connors et al. 2004; Cole et al. 2005; Besla et al. 2012).

These peaks may have implications for the dynamical history of the two systems. In the simplest two body interpretation, the SMC's SFH suggests that the SMC and LMC have been bound for at least the past ~ 9 Gyr, i.e. the age of the first peak, with an orbital period of ~ 4.5 Gyr, i.e. the time of the second peak. However, simulations suggest that it is unlikely for a MC-like pair to be stable for more than ~ 5 Gyr (e.g., Bekki & Chiba 2005; Diaz & Bekki 2012). Further, observational studies find that SMC-LMC-Milky Way triplets are exceedingly rare in the Local Volume (e.g., Liu et al. 2011; Robotham et al. 2012), although LMC-Milky Way pairs appear slightly more common (e.g., Tollerud et al. 2011). Taken at face value, it appears that the enhancements in the intermediate age SFH of the SMC are either unrelated to the long term dynamical history of the MCs or that the MCs are extreme outliers in the timescale distribution of stable binary systems. In the case of the former, the origin of the seemingly periodic star formation enhancements in the SMC is unclear, while for the latter, a long lived SMC-LMC binary is somewhat easier to explain if the pair had a late infall time.

A third clear SFH feature is the increase in star formation in both galaxies ~ 3.5 Gyr ago, presumably due to the gravitational influence of the Milky Way (e.g., Murai & Fujimoto 1980; Gardiner et al. 1994; Bekki & Chiba 2005). These strong increases in star formation activity are unprecedented in either galaxy, suggesting that this is an episode likely due to a first close passage with the Milky Way, as opposed to a history of repeated orbits. Subsequent interactions between the two MCs may have triggered smaller peaks in the SFH of the SMC and/or transferred stars and gas between the systems (e.g., Olsen et al. 2011; Besla et al. 2012).

Finally, we connect the variations in the SFHs of individual fields to putative historical interaction scenarios of the galaxy pair. The presence of age gradients in the SMC (e.g., Gardiner & Hatzidimitriou 1992; Zaritsky et al. 2000; Sabbi et al. 2009) and LMC (e.g., Harris & Zaritsky 2009; Saha et al. 2010; Piatti et al. 2012) are well-documented. In the case of the SMC, our SFHs show similar behavior to previous studies. Namely, at ~ 3.5 Gyr ago, star formation in the SMC has shut off in the outer regions and sharply increased in the inner regions. One interpretation is that the gas supply of the lower mass SMC was funneled into the center of the galaxy, presumably due to an interaction with the more massive LMC. Models suggest that the MCs were ~ 500 kpc from the Milky Way 3.5 Gyr ago (e.g., Besla et al. 2007), making other physical effects such as ram pressure stripping less likely. Alternatively, our outer SMC fields may in fact simply be probing the older 'halo' population of the

SMC (e.g., Nidever et al. 2011). Overall, the uncertainties in the geometry of the SMC, i.e., edge-on vs. face-on, and the small number of fields considered in this preliminary study make it challenging to causally interpret spatial SFH variations in the SMC.

In both galaxies, our fields do not extend to the ‘halo’ fields. At such large galactocentric distances, the stellar crowding is typically minimal and deep CMDs can be constructed from ground based imaging (e.g., Noël et al. 2009; Saha et al. 2010). As a result of our disk biased spatial coverage the population gradient we find in the SMC and lack of population gradient in the LMC are not globally representative. Completed analysis of the full complement of archival fields will significantly expand the extent of the HST spatial coverage, relative to this study, and allow us to explore the connection between global and spatially-varying SFHs scenarios in greater detail.

5 SUMMARY

We have presented preliminary results from an HST archival program aimed at constraining the ancient field population SFHs of the MCs (HST-AR-12853; PI. D. Weisz). To demonstrate the quality of the data and preview results of the full program, we have plotted the CMDs 7 spatially diverse fields in the SMC and 8 fields in the LMC and used an identical CMD fitting technique to derive the SFHs of each field. From the SFHs of the individual fields, we computed the mass weighted average SFH for each galaxy, and found them to be in good agreement with those from previous studies. From the average SFHs we found that (1) for ages > 12 Gyr, both galaxies exhibit star formation consistent with a constant lifetime SFH, suggesting either suppressed or under-fueled star formation, relative to other Milky Way satellites at comparable distances; (2) the LMC shows enhanced mass growth from ~ 10 -12 Gyr ago relative to the SMC; (3) the SMC shows distinct peaks in its SFH ~ 4.5 and 9 Gyr, which may be due to periodic encounters with the LMC, while the LMC had roughly constant star formation at the same epochs. Assuming this is an interaction drive feature, it implies an interaction history that has persisted for at least 9 Gyr; (4) at ~ 3.5 Gyr ago both galaxies show a sharp increase in SFR, and their SFHs track each other subsequently, consistent with suggestions of a close encounter with the Milky Way at recent times; (5) Starting around ~ 3.5 Gyr ago, the SF in the outer regions of the SMC abruptly ceases, while the SFR in the galaxy’s center sharply increases, suggesting gas from the outer regions has been centrally funneled. Interpretation of this finding is somewhat complicated to uncertainties in the geometry of the SMC. In contrast, the LMC shows only small spatial variations in its SFH over the radial extent covered by our HST fields. In both cases, our interpretation of spatial trends is limited by the disk-biased spatial coverage of the HST fields considered in this paper. Our planned analysis of > 100 HST archival fields will increase the radial coverage, enabling more secure statements about spatial variations in the SFHs of the MCs and more detailed comparisons with various MC evolutionary models.

ACKNOWLEDGEMENTS

The authors would like to thank the anonymous referee for insightful comments that helped improve the scope and clarity of this paper. The authors would also like to thank Gurtina Besla for her close reading of the manuscript and helpful comments on the current state of Magellanic Cloud evolutionary models. Support for this work was provided by NASA through grant number HST GO-12853 from the Space Telescope Science Institute, which is operated by AURA, Inc., under NASA contract NAS5-26555. This research made extensive use of NASA’s Astrophysics Data System Bibliographic Services.

REFERENCES

- Bekki, K., & Chiba, M. 2005, MNRAS, 356, 680
 Besla, G., Kallivayalil, N., Hernquist, L., et al. 2007, ApJ, 668, 949
 Besla, G., Kallivayalil, N., Hernquist, L., et al. 2010, ApJL, 721, L97
 Besla, G., Kallivayalil, N., Hernquist, L., et al. 2012, MNRAS, 421, 2109
 Bono, G., Caputo, F., Fiorentino, G., Marconi, M., & Musella, I. 2008, ApJ, 684, 102
 Carrera, R., Gallart, C., Hardy, E., Aparicio, A., & Zinn, R. 2008, AJ, 135, 836
 Carrera, R., Gallart, C., Aparicio, A., et al. 2008, AJ, 136, 1039
 Cignoni, M., Cole, A. A., Tosi, M., et al. 2012, ApJ, 754, 130
 Cole, A. A., Tolstoy, E., Gallagher, J. S., III, & Smecker-Hane, T. A. 2005, AJ, 129, 1465
 Cole, A. A., Skillman, E. D., Tolstoy, E., et al. 2007, ApJL, 659, L17
 Connors, T. W., Kawata, D., Maddison, S. T., & Gibson, B. K. 2004, PASA, 21, 222
 da Costa, G. S. 2002, Extragalactic Star Clusters, 207, 83
 de Jong, J. T. A., Yanny, B., Rix, H.-W., Dolphin, A. E., Martin, N. F., & Beers, T. C. 2010, ApJ, 714, 663
 Diaz, J. D., & Bekki, K. 2012, ApJ, 750, 36
 Dolphin, A. E. 2000, PASP, 112, 1383
 Dolphin, A. E., Walker, A. R., Hodge, P. W., et al. 2001, ApJ, 562, 303
 Dolphin, A. E. 2002, MNRAS, 332, 91
 Dolphin, A. E., Weisz, D. R., Skillman, E. D., & Holtzman, J. A. 2005, arXiv:astro-ph/0506430
 Dolphin, A. E. 2012, ApJ, 751, 60
 Fich, M., & Tremaine, S. 1991, ARA&A, 29, 409
 Gallart, C., Zoccali, M., & Aparicio, A. 2005, ARA&A, 43, 387
 Gardiner, L. T., & Hatzidimitriou, D. 1992, MNRAS, 257, 195
 Gardiner, L. T., Sawa, T., & Fujimoto, M. 1994, MNRAS, 266, 567
 Geha, M. C., Holtzman, J. A., Mould, J. R., et al. 1998, AJ, 115, 1045
 Girardi, L., Williams, B. F., Gilbert, K. M., et al. 2010, ApJ, 724, 1030
 Gordon, K. D., Meixner, M., Meade, M. R., et al. 2011, AJ, 142, 102

- Harris, J., Zaritsky, D., & Thompson, I. 1997, *AJ*, 114, 1933
- Harris, J., & Zaritsky, D. 2004, *AJ*, 127, 1531
- Harris, J., & Zaritsky, D. 2009, *AJ*, 138, 1243
- Haschke, R., Grebel, E. K., Duffau, S., & Jin, S. 2012, *AJ*, 143, 48
- Haschke, R., Grebel, E. K., & Duffau, S. 2012, *AJ*, 144, 106
- Haschke, R., Grebel, E. K., & Duffau, S. 2012, *AJ*, 144, 107
- Heller, P., & Rohlfs, K. 1994, *A&A*, 291, 743
- Holtzman, J. A., Hester, J. J., Casertano, S., et al. 1995, *PASP*, 107, 156
- Holtzman, J. A., Gallagher, J. S., III, Cole, A. A., et al. 1999, *AJ*, 118, 2262
- Holtzman, J. A., Afonso, C., & Dolphin, A. 2006, *ApJS*, 166, 534
- Jarosik, N., Bennett, C. L., Dunkley, J., et al. 2011, *ApJS*, 192, 14
- Kallivayalil, N., van der Marel, R. P., Alcock, C., et al. 2006, *ApJ*, 638, 772
- Kallivayalil, N., van der Marel, R. P., & Alcock, C. 2006, *ApJ*, 652, 1213
- Kerber, L. O., Girardi, L., Rubele, S., & Cioni, M.-R. 2009, *A&A*, 499, 697
- Kim, S., Staveley-Smith, L., Dopita, M. A., et al. 1998, *ApJ*, 503, 674
- Kroupa, P. 2001, *MNRAS*, 322, 231
- Lin, D. N. C., & Lynden-Bell, D. 1982, *MNRAS*, 198, 707
- Lin, D. N. C., Jones, B. F., & Klemola, A. R. 1995, *ApJ*, 439, 652
- Liu, L., Gerke, B. F., Wechsler, R. H., Behroozi, P. S., & Busha, M. T. 2011, *ApJ*, 733, 62
- McCumber, M. P., Garnett, D. R., & Dufour, R. J. 2005, *AJ*, 130, 1083
- Meixner, M., Gordon, K. D., Indebetouw, R., et al. 2006, *AJ*, 132, 2268
- Meixner, M., Galliano, F., Hony, S., et al. 2010, *A&A*, 518, L71
- Murai, T., & Fujimoto, M. 1980, *PASJ*, 32, 581
- Nidever, D. L., Majewski, S. R., Muñoz, R. R., et al. 2011, *ApJL*, 733, L10
- Noël, N. E. D., & Gallart, C. 2007, *ApJL*, 665, L23
- Noël, N. E. D., Aparicio, A., Gallart, C., et al. 2009, *ApJ*, 705, 1260
- Olsen, K. A. G. 1999, *AJ*, 117, 2244
- Olsen, K. A. G., Zaritsky, D., Blum, R. D., Boyer, M. L., & Gordon, K. D. 2011, *ApJ*, 737, 29
- Pagel, B. E. J., & Tautvaisiene, G. 1998, *MNRAS*, 299, 535
- Piatti, A. E., Santos, J. F. C., Jr., Clariá, J. J., et al. 2005, *A&A*, 440, 111
- Piatti, A. E., Geisler, D., & Mateluna, R. 2012, *AJ*, 144, 100
- Rubele, S., Kerber, L., Girardi, L., et al. 2012, *A&A*, 537, A106
- Sabbi, E., Gallagher, J. S., Tosi, M., et al. 2009, *ApJ*, 703, 721
- Robotham, A. S. G., Baldry, I. K., Bland-Hawthorn, J., et al. 2012, *MNRAS*, 424, 1448
- Saha, A., Olszewski, E. W., Brondel, B., et al. 2010, *AJ*, 140, 1719
- Skillman, E. D., Tolstoy, E., Cole, A. A., et al. 2003, *ApJ*, 596, 253
- Smecker-Hane, T. A., Cole, A. A., Gallagher, J. S., III, & Stetson, P. B. 2002, *ApJ*, 566, 239
- Stanimirović, S., Staveley-Smith, L., & Jones, P. A. 2004, *ApJ*, 604, 176
- Tollerud, E. J., Boylan-Kolchin, M., Barton, E. J., Bullock, J. S., & Trinh, C. Q. 2011, *ApJ*, 738, 102
- Tolstoy, E., Hill, V., & Tosi, M. 2009, *ARA&A*, 47, 371
- Udalski, A., Soszynski, I., Szymanski, M. K., et al. 2008, *ACTAA*, 58, 89
- Udalski, A., Soszyński, I., Szymański, M. K., et al. 2008, *ACTAA*, 58, 329
- Weisz, D. R., Dalcanton, J. J., Williams, B. F., et al. 2011, *ApJ*, 739, 5
- Zaritsky, D., Harris, J., & Thompson, I. 1997, *AJ*, 114, 1002
- Zaritsky, D., Harris, J., Grebel, E. K., & Thompson, I. B. 2000, *ApJL*, 534, L53
- Zaritsky, D., Harris, J., Thompson, I. B., Grebel, E. K., & Massey, P. 2002, *AJ*, 123, 855

This paper has been typeset from a \TeX / \LaTeX file prepared by the author.